

Equivalent Circuit Model for InP-based Uni-Traveling-Carrier Photodiodes with Dipole-doped Structure

Q. Q. Meng^{1*}, H. Wang^{1,2}, B. Gao^{1,3}, C. Y. Liu¹, K. S. Ang¹, X. Guo¹, and J. Gao⁴

1. Temasek Laboratories@NTU (TL@NTU), Nanyang Technological University, 50 Nanyang Drive, Singapore 637553

2. School of Electrical and Electronic Engineering, Nanyang Technological University, Nanyang Avenue, Singapore 639798

3. School of Electronic and Information Engineering, Xi'an Jiaotong University, No.28 Xianning West Road, Xi'an 710049, China

4. School of Information Science and Technology, East China Normal University, No. 500 Dongchuan Road, Shanghai 200262, China

*: Corresponding author, E-mail: qqmeng@ntu.edu.sg

Abstract: An equivalent circuit model has been proposed to analyze the high performance of InP-based uni-traveling-carrier photodiodes (UTC-PDs) with novel dipole-doped structure. The validity of this model has been confirmed with experimental data.

OCIS codes: (230.5160) Photodetectors; (230.5170) Photodiodes

1. Introduction

Uni-travelling-carrier photodiodes (UTC-PDs) [1] with high-photocurrent and high-speed performance have attracted intensive research interests due to their wide applications in high-performance microwave or millimeter-wave photonic systems [2, 3]. Typically, in a UTC-PD with a p-type doped InGaAs absorption layer and a wide n-type doped InP collector, InGaAsP compositional graded quaternary structures are employed at the InGaAs/InP absorption/collection interface to smooth the bandgap discontinuity, suppress the current blocking, and improve the device performance. However, the introduction of compositional graded InGaAsP layers could result in the complexity and difficulty in material growth and subsequent device fabrication. The use of dipole-doped structure, which eliminates the quaternary layers, may ease the epi-layers growth and device fabrication without compromising device performance. Recently, UTC-PDs with novel dipole-doped structure have been demonstrated with high-photocurrent and high-speed performance by us [4].

In order to predict and analyze the performance of PDs, various modeling methods have been investigated such as numerical modeling and equivalent circuit modeling. Physic-based equivalent-circuit models of PDs are usually convenient to apply with the use of computer-aided simulation software. However, most of the reported equivalent circuit models are designed for p-i-n photodiodes [5-8] and few can be accurately applied in UTC-PDs due to the different operation mechanism between p-i-n PDs and UTC-PDs.

In this work, an equivalent circuit model for UTC-PDs with novel dipole-doped structure has been developed to predict and analyze the high-speed performance. This model is built based on the actual device structure and physics of dipole-doped UTC-PDs. The dipole-doped structure at the InGaAs/InP heterostructure interface is incorporated in the equivalent circuit model to simulate its effectiveness on reducing the current blocking. The results for a 12- μm -diameter UTC-PD with a large 3-dB bandwidth of 62.5 GHz is presented.

2. Device Structure and Measurement

The major difference in epi-layer structure between conventional UTC-PD and our UTC-PD with dipole-doped structure is at the InGaAs/InP absorption/collection hetero interface. The abrupt energy barrier at InGaAs/InP absorption/collection interface can block electron flow, cause a buildup of stored charge, degrade DC performance at high current densities and also limit the high-speed performance. To overcome this problem, compositional graded InGaAsP layers were normally inserted between the InGaAs absorption and InP collection layers [3, 9]. However, this often results in the difficulty of material growth and the complexity of device fabrication.

In our UTC-PD structure, which is shown in Table 1, novel dipole-doped layers, in combination with a 22-nm-thick undoped InGaAs setback layer were employed at the InGaAs/InP absorption/ collection interface to reduce the current blocking effect. The dipole-doped layers consist of an 8-nm-thick InGaAs layer and an 8-nm-thick InP layer, both of which have been p- and n-type doped with the concentration of $1 \times 10^{18} \text{ cm}^{-3}$.

Top-illuminated UTC-PDs with cylindrical mesas of different diameters varied from 12 to 80 μm were fabricated using standard processing techniques. The mesa formation was based on wet etching processes to minimize the surface damage. The mesa was connected to the coplanar waveguide for RF probing with BCB planarization. The responsivity and high speed response characteristics of the fabricated dipole-doped UTC-PDs have been tested by using an Agilent Lightwave Component Analyzer (LCA) in the frequency range from 10 MHz to 20 GHz, incorporated with an Erbium Doped Fibre Amplifier (EDFA). Both wide bandwidth of more than 20GHz

(limitation of measurement equipment) and high photocurrent of 160 mA have been achieved from our UTC-PDs with dipole-doped structure [4].

Table 1 Epi-layer structure of UTC-PD with dipole-doped structure.

In _{0.6} Ga _{0.4} As, p+, 1×10 ¹⁹ cm ⁻³ , 30 nm
InP, p+, 1×10 ¹⁹ cm ⁻³ , 200nm
In _{0.53} Ga _{0.47} As, p+, 2×10 ¹⁸ cm ⁻³ , 50 nm
In _{0.53} Ga _{0.47} As, p+, 1×10 ¹⁸ cm ⁻³ , 100 nm
In _{0.53} Ga _{0.47} As, p+, 5×10 ¹⁷ cm ⁻³ , 300 nm
In _{0.53} Ga _{0.47} As, undoped, 22 nm
In _{0.53} Ga _{0.47} As, p+, 1×10 ¹⁸ cm ⁻³ , 8 nm
InP, n+, 1×10 ¹⁸ cm ⁻³ , 8 nm
InP, n+, 1×10 ¹⁷ cm ⁻³ , 13 nm
InP, n+, 5×10 ¹⁶ cm ⁻³ , 200 nm
In _{0.53} Ga _{0.47} As, n+, 5×10 ¹⁸ cm ⁻³ , 30 nm
InP, n+, 5×10 ¹⁸ cm ⁻³ , 600 nm
InP, semi-insulating substrate

3. Equivalent Circuit Model of InP UTC-PDs with Dipole-doped Structure

Figure 1 shows the equivalent circuit model of the InP-based UTC-PD with dipole-doped structure. All the equivalent circuit components are connected and related to the physical parameters of UTC-PD.

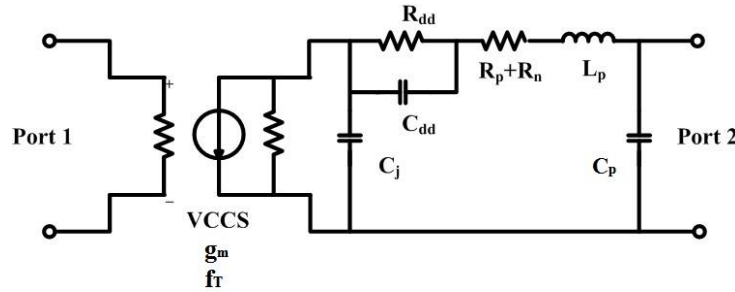


Fig. 1 Equivalent circuit model of UTC-PD with dipole-doped structure.

The optical part of port 1 is combined in parallel to a voltage-controlled current source (VCCS). g_m is the transconductance, and $f_T = 1/(2\pi\tau_T)$ where τ_T is the electron transit time. In the proposed model, R_p and R_n represent the UTC-PD resistance of p type absorption layer and n type collection layer, respectively; C_j is the junction capacitance; C_p is the pad capacitance; L_p is the pad inductance. R_{dd} and C_{dd} represent the resistance and capacitance of the dipole-doped structure.

4. Results and Discussion

Figure 2 shows simulated and measured S_{22} parameters from a 12- μm -diameter dipole-doped UTC-PD under -5 V reverse bias voltage with optical input power of 100 mW. Fig. 3 shows simulated and measured frequency responses (S_{21}) from a 12- μm -diameter dipole-doped UTC-PD under -2 V and -5 V bias with optical input power of 100 mW. As shown in these two figures, by carefully choosing the values for the circuit components in Fig. 1, the simulated data can match the measured data very well in the frequency range from 10MHz to 20GHz. The best curve fitting demonstrates the validity of proposed equivalent circuit model. In Fig.3, the device exhibits a large 3-dB bandwidth, which is far beyond 20 GHz (limitation of measurement equipment) and it is estimated to be around 62.5 GHz with the equivalent circuit model when the reverse bias is -5 V.

The key modeling procedure can be summarized as follow. First, values of C_j , C_p , L_p , R_p , R_n , R_{dd} and C_{dd} in the equivalent circuit in Fig. 1 are determined by fitting modeled S_{22} parameters to measured S_{22} parameters in the frequency range from 10MHz to 20GHz as shown in Fig.2. Then, the g_m and f_T are obtained by matching the simulated frequency response (S_{21}) to the measured frequency response (S_{21}) in Fig.3. Extracted values for the

equivalent circuit model parameters are summarized in Table 2. When the reverse bias increase from -2 V to -5 V, The increase of f_T and decrease of C_j , with the increase of reverse bias -2 V to -5 V can be explained by depleting the collector layer and shortening the electron transit time at high electric field,

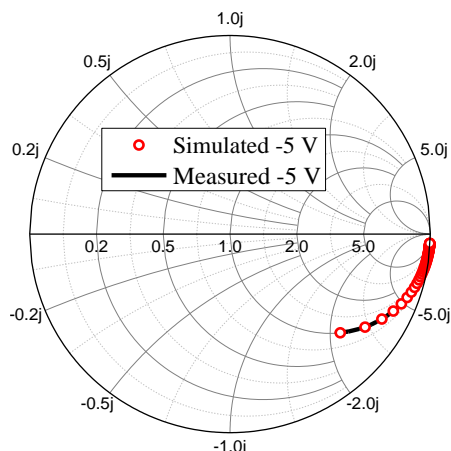


Fig. 2 Measured (line) and simulated (symbols) S_{22} parameter of a 12- μm -diameter UTC-PD with dipole-doped structure under -5 V bias when the optical input power is 100 mW.

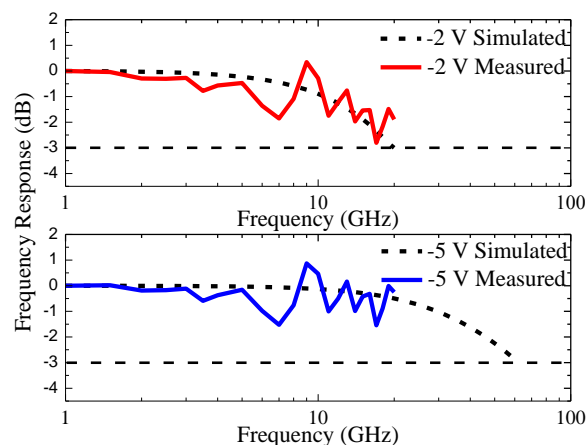


Fig. 3 Measured (solid line) and simulated (dashed line) frequency response (S_{21}) of a 12- μm -diameter UTC-PD with dipole-doped structure under -2V and -5 V bias when the optical input power is 100 mW.

Table 2 Extracted parameter values.

V_{RB}	C_j (pF)	C_p (fF)	L_p (pH)	$R_p + R_n$ (Ω)	R_{dd} (Ω)	C_{dd} (pF)	g_m (S)	f_T (GHz)
-2 V	0.038	32.5	120	36	14	2	0.01	30
-5 V	0.029	32.5	120	31	8	2	0.01	100

5. Conclusions

In summary, an equivalent circuit model of InP-based UTC-PD with dipole-doped structure at the InGaAs/InP absorption/collection interface is proposed. Particular attention has been paid by taking the dipole-doped layer into the consideration for the model. The effectiveness of the model has been validated by modeling a 12- μm -diameter UTC-PD with dipole-doped structure under different reverse bias. A large 3-dB bandwidth of 62.5 GHz has been predicted.

6. References

- [1] T. Ishibashi, N. Shimizu, S. Kodama, H. Ito, T. Nagatsuma, and T. Furuta, "Uni-traveling-carrier photodiodes," presented at the Tech. Dig. Ultrafast Electronics and Optoelectronics, OSA Spring Topical Meeting, (1997).
- [2] K. Kato, "Ultrawide-band/high-frequency photodetectors," *IEEE Trans. Microw. Theory Tech.* **47**, 1265-1281 (1999).
- [3] H. Ito, S. Kodama, Y. Muramoto, T. Furuta, T. Nagatsuma, and T. Ishibashi, "High-speed and high-output InP-InGaAs untraveling-carrier photodiodes," *IEEE J. Sel. Top. Quantum Electron.* **10**, 709-727 (2004)
- [4] Q. Q. Meng, H. Wang, C. Y. Liu, K. S. Ang, X. Guo, B. Gao, Y. Tian, C. M. M. Kumar, and J. Gao, "High-Photocurrent and Wide-Bandwidth UTC Photodiodes with Dipole-Doped Structure," accepted by *IEEE Photonics Technol. Lett.* (2014).
- [5] G. Lucovsky, R. B. Emmons, and R. F. Schwarz, "Transit-Time Considerations in P-I-N Diodes," *J. Appl. Phys.* **35**, 622 (1964).
- [6] J. M. Zhang and D. R. Conn, "State-space modeling of the PIN photodetector," *J. Lightwave Technol.* **10**, 603-609 (1992).
- [7] J. Jau-Ji, L. Cheng-Kuang, H. Chien-Mei, L. Huang-Hsiang, and L. Hsiu-Chih, "Time-delay circuit model of high-speed p-i-n photodiodes," *IEEE Photonics Technol. Lett.* **14**, 525-527 (2002).
- [8] G. Wang, T. Tokumitsu, I. Hanawa, Y. Yoneda, K. Sato, and M. Kobayashi, "A time-delay equivalent-circuit model of ultrafast p-i-n photodiodes," *IEEE Trans. Microw. Theory Tech.* **51**, 1227-1233 (2003).
- [9] N. Li, X. Li, S. Demiguel, X. G. Zheng, J. C. Campbell, D. A. Tulchinsky, K. J. Williams, T. D. Isshiki, G. S. Kinsey, and R. Sudharsanan, "High-saturation-current charge-compensated InGaAs-InP uni-traveling-carrier photodiode," *IEEE Photonics Technol. Lett.* **16**, 864-866 (2004).